# Original Article
# Epithelioid angiomyolipoma of the kidney: CT and CEUS characteristics and clinical outcomes

Dong-Wei Yao[1], Cheng Liu[1], Xue-Jun Liu[1], Duo Liu[1], Qing Zhang[2], Wei Wang[2], Guang-Xiang Liu[2], Xiao-Zhi Zhao[2], Hong-Qian Guo[2]

[1]Department of Urology, The Second People's Hospital of Lianyungang, Lianyungang, Jiangsu, China; [2]Department of Urology, Nanjing Drum Tower Hospital, The Affiliated Hospital of Nanjing University Medical School, Nanjing, Jiangsu, China

**Abstract:** Objective: To review the computed tomography (CT) and contrast-enhanced ultrasonography (CEUS) features and clinical outcomes of renal epithelioid angiomyolipomas (EAMLs). Materials and methods: Seventeen patients diagnosed with EAML from January 2004 to June 2015 at the Second People's Hospital of Lianyungang and Nanjing Drum Tower Hospital were included. All of the patients underwent CT, and six underwent CEUS. Patient demographics, outcomes, imaging characteristics and pathologic features were determined by chart review. Results: The patients included seven women and ten men with a mean age 45.7 (range, 23-62) years. Only two patients had tuberous sclerosis complexes (TSCs). Seven patients presented with flank pain, one presented with acute bleeding, and nine were asymptomatic. Nine patients underwent radical nephrectomy, and eight patients underwent partial nephrectomy. The mean follow-up period was 28.5 (range, 2-126) months, and fifteen patients were alive with no evidence of disease at the time of the last follow-up, one patient exhibited local recurrence and lung metastases, and another patient developed distant metastasis. The mean maximal tumor diameter was 6.1 (range, 1.2-12.5) cm. The fat components of two lesions were detected by CEUS and one by CT. On unenhanced CT, the intratumoral attenuations were hyperattenuating in nine patients, isoattenuating in one patient and hypoattenuating in seven patients. The contrast enhancement degree was mild in one patient, moderate in six patients and marked in ten patients. The contrast enhancement pattern was homogeneous in eight lesions and heterogeneous in nine lesions. On CEUS analysis, two lesions were found to be homogeneous, and four were heterogeneous. Tumor necrosis was observed in six cases, five of which had a maximal tumor diameter ≥ 10 cm, and hemorrhaging was present in three cases. All patients were positive for melanoma (twelve were positive for HMB45, three were positive for melan A, and two were positive for both). Conclusions: Renal EAML can have a range of imaging appearances. Our data suggested that the majority of the tumors (size < 10 cm) were solid and had a tendency to be hyperattenuating on unenhanced CT images. Hemorrhaging or necrosis was observed in tumors with sizes ≥ 10 cm with heterogeneous enhancement. Regarding CEUS appearances, the uniform lesions were hypervascular and homogeneous, whereas the lesions that contained hemorrhaging, necrosis or fat components were heterogeneous. In contrast to classic AML, which is benign, EAML is potentially malignant and exhibits aggressive clinical features, including local recurrence and distant metastasis.

Keywords: Kidney, epithelioid angiomyolipoma, computed tomography, ultrasonography, outcome

## Introduction

Classic renal angiomyolipoma (AML) is a benign mesenchymal neoplasm composed of a variable proportion of adipose tissue, spindle smooth muscle cells, and dysmorphic blood vessels [1]. AML has been classified under the group of perivascular epithelioid cell tumors (PEComas) [2] that also includes renal and hepatic angiomyolipomas, clear cell sugar tu-

mors of the lung, pulmonary lymphangioleiomyomatosis, and clear cell myomelanocytic tumors of the falciform ligamentum teres [3]. PEC tumors exhibit co-expression of both melanocytic (HMB-45, Melan-A) and smooth muscle (actin, desmin) markers [4]. Epithelioid AMLs (EAMLs) were first reported in 1997 by Eble et al. [5] and are composed of polygonal cells with clear to eosinophilic cytoplasm and round to oval nuclei that may exhibit varying degree

**Table 1.** Clinical features and outcomes of 17 patients with EAML

| Features | Patients had CT (n=17) | Patients had both CT and CEUS (n=6) |
|---|---|---|
| Mean age at surgery (y) | 45.7 (23-62) | 44.2 (22-59) |
| Gender | | |
|     Male | 10 | 3 |
|     Female | 7 | 3 |
| Tuberous sclerosis complex (TSC) | | |
|     Absent | 15 | 5 |
|     Present | 2 | 1 |
| Present symptoms | | |
|     Flank pain | 7 | 3 |
|     Acute bleeding | 1 | 0 |
|     Asymptomatic | 9 | 3 |
| Surgery | | |
|     Radical nephrectomy | 9 | 4 |
|     Partial nephrectomy | 8 | 2 |
|     Mean follow-up (mo) | 28.5 (2-126) | 17.5 (8-40) |
| Clinical outcomes | | |
|     Recurrence and Metastasis | 1 (retroperitoneal, lung) | 1 (retroperitoneal, lung) |
|     Metastasis | 1 (adrenal gland) | 1 (adrenal gland) |
|     No evidence of disease | 15 | 4 |

of nuclear atypia [1]. This rare subtype of AML may exhibit aggressive biology, including recurrence and metastasis [2, 6]. The 2004 World Health Organization classification of tumors defines epithelioid angiomyolipomas of the kidney as potentially malignant mesenchymal neoplasms with reported metastases in approximately one-third of cases [7]. However, this conclusion was based primarily on individual case reports and small retrospective series, and recent studies have demonstrated that the rate of aggressive clinical behavior is lower than that previously reported [1, 7, 8].

The imaging appearances of EAMLs have been much less well reported than the histopathologic features [9-12]. Herein, we retrospectively reviewed EAML imaging findings obtained with CT and CEUS. We wish to provide useful clues to distinguish EAMLs from benign tumors because of the malignant potential of EAMLs.

**Materials and methods**

*Patients*

Institutional review board approval was obtained to retrospectively review images and surgical pathology files. Between January 2004 and June 2015, seventeen patients were pa-

thologically diagnosed with an EAML of the kidney at our institutions. All of the patients' medical records, including age, gender, TSC, symptoms, surgery, follow-up, and clinical outcomes, were retrospectively reviewed and summarized.

*Pathological diagnosis*

A pathologist with 12 years of experience in genitourinary pathology at the Nanjing Drum Tower Hospital made the diagnoses of EAML according to the 2004 WHO classification, which defines an EAML as a proliferation of predominantly round to polygonal epithelioid cells with enlarged vesicular nuclei and often with prominent nucleoli. The tumors were analyzed with respect to the tumor configuration, hemorrhaging, and necrosis, and the available immunohistochemical stains were reviewed.

*CT technique*

All the pre-operative images were obtained using a helical CT (Philips Brilliance, Holland). Unenhanced, cortico-medullary, nephrographic, and excretory phase images were obtained through the kidneys with scan delays of 30 s, 90 s and 300 s after administration. The section thicknesses ranged from 1.5 to 3 mm, and
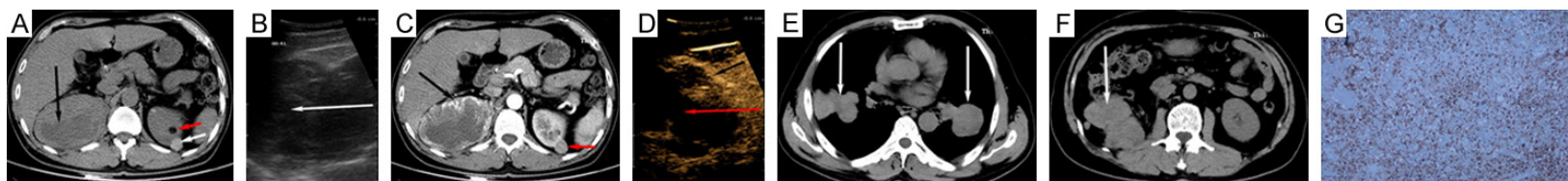
**Figure 1.** A 59-year-old man with a tuberous sclerosis complex. A. Unenhanced CT showing a 10.2-cm cyst-solid mass in the upper pole of the right kidney (black arrow). A small conventional fat-containing angiomyolipoma (red arrow) and a hyperattenuating mass were observed in the left kidney (white arrow). B. A heterogeneous mass in the upper pole of the right kidney was detected on conventional sonography (white arrow). C. Dynamic enhanced CT showing a heterogeneously enhanced tumor in the corticomedullary phase (black arrow), and the solid tumor in the left kidney was markedly enhanced but was hypoattenuating relative to the renal cortex. D. On CEUS, the tumor was heterogeneously enhanced (black and red arrows). E. CT scan 7 months after nephrectomy showing lung metastases (white arrows). F. A retroperitoneal neoplasm measuring up to 12.5 cm was detected, which suggested local recurrence. G. The tumor cells were positive for HMB45 antibody (original magnification × 100).

**Table 2.** Imaging characteristics of the 17 cases of EMAL

| Characteristics | Patients had CT (n=17) | Patients had both CT and CEUS (n=6) |
|---|---|---|
| Mean size (cm) | 6.1 (1.2-12.5) | 6.9 (1.2-11.3) |
| CT finding of fat | | |
|    Absent | 16 | 5 |
|    Present | 1 | 1 |
| CEUS finding of fat | | |
|    Absent | | 4 |
|    Present | | 2 |
| Unenhanced CT appearances | | |
|    Hyperattenuating | 9 | 4 |
|    Isoattenuating | 1 | 0 |
|    Hypoattenuating | 7 | 2 |
| Enhanced CT appearances | | |
|    Mild enhancement | 1 | 0 |
|    Moderate enhancement | 6 | 2 |
|    Marked enhancement | 10 | 4 |
|    Homogeneous enhancement | 8 | 3 |
|    Heterogeneous enhancement | 9 | 3 |
| CEUS appearances | | |
|    Homogeneous | | 2 |
|    Heterogeneous | | 4 |

the reconstruction intervals ranged from 0.5 to 1.5 mm. Intravenous injections of non-ionic contrast medium of 300 mg iodine per milliliter (Omnipaque, GE Healthcare) were administered (volume 85 ml; injection rate 3 ml/s via a mechanical power injector) and followed by a 20-ml saline flush via an 18-gauge catheter. The CT densities were measured in representative portions of the masses that did not have necrosis on unenhanced and contrast imaging.

*CEUS technique*

An abdominal ultrasound (US) was performed first, and color Doppler US was performed prior to the operation to detect the arterial blood flow in and around the tumor. The Doppler parameters were optimized to detect slow flow velocities with a pulse repetition frequency of 700 Hz, a medium wall filter, and low-velocity flow optimization. The color gain was increased until the color noise was evident and then lowered slightly to clean the image. Contrast-enhanced ultrasonography with low acoustic US pressure (2-4 MHz transducer; mechanical index < 0.1; 12-13 frame rate/s) was performed utilizing a 2202-UV ultrasonography device (BK Medical, Copenhagen, Dan-

mark). A dose of 1.2 ml of sulphur hexafluoride in the form of micro-bubbles (SonoVue, Bracco, Milan, Italy) was intravenously injected as a rapid bolus via an antecubital vein using a 20-gauge cannula. This injection was followed by a 5-ml saline flush. Additionally, while the patients held their breath after the contrast appeared on the imaging, CEUS was performed with a focus on the mass area. All examinations were recorded on a magneto-optical disk system for further analysis.

*Imaging analysis*

A senior internist with 9 years of experience in urinary system CEUS and who was blinded to the CECT results reviewed the CEUS studies. Moreover, a senior radiologist with 11 years of experience in renal imaging who was also blinded to the CEUS results reviewed the CT studies. The tumor size, laterality, location, existence of fat, attenuating value, heterogeneity, and the degree of enhancement were evaluated. The measurement of the CT attenuation was performed using the highest CT attenuation area to avoid obtaining data from necrotic or cystic areas using a reviewer-defined region of interest. Based on the unenhanced CT findings, the tumors were classified as hyperattenuating, isoattenuating or hypoattenuating based on comparisons with the renal parenchyma (cortex). Homogeneity was defined by an area of more than 90% with the same attenuation value as ascertained by visual inspection [11]. According to previous studies [13-19], the degree of enhancement of the hypervascular clear cell type RCC was 90-149 HU, and that of hypovascular papillary RCC was 15-56 HU. Thus, enhancements greater than 90 HU were classified as marked enhancements, those between 60 and 90 HU were classified as moderate enhancements, and those less than 60 HU were classified mild enhancements.

**Results**

*Clinical information*

**Table 1** summarizes the clinical features and outcomes of EAML patients. The mean age at
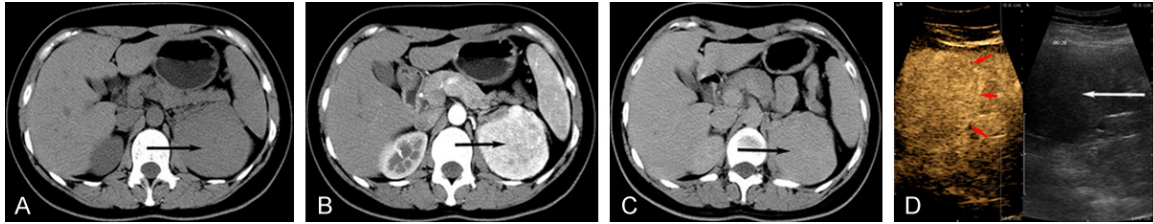
**Figure 2.** A 35-year-old woman with a homogeneous solid-type lesion. (A) Unenhanced CT showing an 8.0-cm hyper-attenuating mass in the upper pole of the left kidney (black arrow). No fat density was detected. Enhanced CT showing a homogenously enhanced tumor in corticomedullary phase (B: Black arrow) and excretory phase images (C: Black arrow). (D) A homogenous mass in the upper pole of the left kidney was detected on conventional sonography (white arrow). On CEUS, the tumor was homogenously enhanced, and the sonographic criterion for the presence of a pseudocapsule sign was a rim of perilesional enhancement (red arrows).
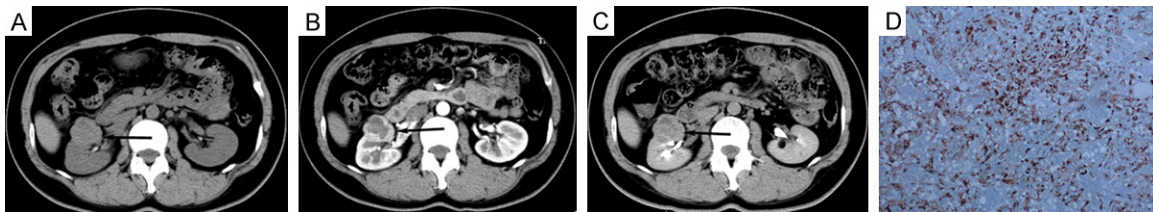


**Figure 3.** A 36-year-old woman with a 3.2-cm solid-type lesion. (A) Unenhanced CT showing a 3.2-cm hyperattenuating mass in the upper pole of the right kidney (black arrow). No fat density was detected. (B) Enhanced CT showing a heterogeneously enhanced tumor in the corticomedullary phase (B: Black arrow) and excretory phase images (C: Black arrow). The tumor exhibited a peripheral enhancement pattern. (D) The tumor cells were positive for HMB45 antibody (original magnification × 200).

surgery was 45.7 years, and the range was 23 to 62 years. Seven patients were females, ten were males, and only two patients had tuberous sclerosis complexes. Seven patients presented with flank pain, one presented with acute bleeding, and nine were asymptomatic. Nine patients underwent radical nephrectomy, and the others underwent partial nephrectomy. The follow-ups of the seventeen cases lasted 2-126 months (mean, 28.5 months). A follow-up CT 7 months after nephrectomy in one case revealed a retroperitoneal neoplasm measuring up to 12.5 cm, which suggested local recurrence, and unenhanced CT also revealed lung metastases (**Figure 1**). Another patient developed a distant metastasis in the adrenal gland, but the lesion had not been biopsied.

*Imaging characteristics*

The imaging characteristics are summarized in **Table 2**. All of the patients underwent CT, and six underwent CEUS. The tumors were located in the left kidneys in six cases and in the right kidneys in eleven. The lesions were located in the upper renal pole in nine cases, the interpolar region in two cases, and the lower renal pole in six cases. The maximum tumor diameters ranged from 1.2 to 12.5 cm (mean 6.1 cm). Fat

components were identifiable with CEUS in two cases and with unenhanced CT in one case. According to the unenhanced CT findings, the CT attenuations of the lesions were hyperattenuating in nine, isoattenuating in one, and hypoattenuating in seven patients. Nine lesions were categorized as heterogeneous, and eight were categorized as homogeneous (**Figure 2**). Six of the nine heterogeneous types were accompanied by hemorrhaging or necrosis in the histopathological specimens, and fat components were found in two. In one of these nine tumors, the lesion was homogeneous on unenhanced CT but was heterogeneously enhanced and exhibited a peripheral enhancement pattern (**Figure 3**). The tumor enhancements ranged from mild (one case) to moderate (six cases) to marked (nine cases). Among the six cases with CEUS findings, two uniform lesions were hypervascular and homogeneous, two were accompanied by hemorrhaging or necrosis, and the two that contained fat components were heterogeneous.

*Pathologic characteristics*

The pathologic findings are summarized in **Table 3**. Eleven lesions were the solid type, and five lesions were the cyst-solid type. Tumor

**Table 3.** Pathologic Characteristics in 17 cases of EMAL

| Characteristics | Patients had CT (n=17) | Patients had both CT and CEUS (n=6) |
|---|---|---|
| Tumor configuration | | |
|   Solid | 11 | 4 |
|   Cyst-solid | 6 | 2 |
|   Hemorrhage | 3 | 1 |
|   Necrosis | 6 | |
|   Size ≥ 10 cm | 5 | 2 |
|   Size < 10 cm | 1 | 0 |
| Immunohistochemistry | | |
|   HMB-45 positive | 12 | 5 |
|   Melan A positive | 3 | 0 |
|   Both | 2 | 1 |

necrosis was observed in six cases, five of which had maximal tumor diameters ≥ 10 cm, and hemorrhaging was present in three cases. All patients were positive for melanoma (twelve were positive for HMB45, three were positive for melan A, and two were positive for both).

## Discussion

EAML is a rare variant of renal AML, which is a potentially malignant neoplasm. Gender is not a factor in the occurrence of EAML, whereas classical AMLs occur predominantly in females with female:male ratios of 4:1 for both sporadic and TSC cases. Sato et al. reviewed 21 previously reported cases and found that both genders were equally likely to be involved (male: female, 11:10) [20]. In our study, the male vs female ratio was 10:7. The analysis of 61,389 AML patients by Fittschen A et al. revealed that the ages of the patients ranged from 1 month to 105 years and included 30,500 females (54.6 ± 18.7 years) and 30,889 males (54.8 ± 18.3 years) [21]. According to Aydin et al. [1] and He et al. [7], the mean ages of EAML patients at presentation are 38.6 years and 49.7 years, respectively, and mean age of our patients was 45.7 years. Thus, it seems that EAML patients are younger than classical AML patients.

Microscopically, EAMLs frequently present with hemorrhaging, necrosis, polygonal cells, nuclear atypia, and mitotic activity. In our series, tumor necrosis was observed in six cases, five of which had maximal tumor diameters ≥ 10 cm. Our findings suggest that large tumor size

(≥ 10 cm) might be accompanied by necrosis. When the epithelioid component predominates and nuclear atypia is prominent, there is often diagnostic difficulty that can contribute to the misdiagnoses of EAMLs as RCCs, metastatic melanomas or sarcomas [5, 22-24]. Indeed, some previously reported RCCs were confirmed to be EAMLs based upon expert reevaluation of immunohistochemical assays [5, 25]. In such situations, the immunohistochemical assays are significant in the differential diagnosis. These tumors are usually positive for one or more melanocytic markers, such as HMB45, melan A or A103, although staining can be focal. These tumors often express smooth muscle markers (particularly SMA and less commonly desmin) and are negative for epithelial markers and S-100. As described by Aydin et al. [1], no melanocytic marker is positive in all EAMLs, but all EAMLs are positive for either HBM-45 or melan A. Therefore, a panel of melanocytic markers has been suggested for use in EAML patients. In our cases, all of the patients were positive for melanoma (twelve were positive for HMB45, three were positive for melan A, and two were positive for both).

Imaging descriptions of EAMLs are relatively rare, and only single cases and small series have been studied with US, CT and/or MR [2, 8-12]. Our seventeen cases exhibited a wide range of imaging characteristics. The appearances ranged from small, well-defined, and homogeneous lesions to large and markedly heterogeneous masses. Hyperattenuation on unenhanced CT might be a characteristic finding of EAML due to the high cellular content and lack of fat in EAMLs. Among our eleven solid cases, the unenhanced CT attenuations were hyperattenuating in nine, isoattenuating in one, and hypoattenuating in one. In a previously reported study by Tsukada et al., the authors also found that six of the seven cases for which unenhanced CT images were available were hyperattenuating, and the remaining case was isoattenuating [11]. The enhancement patterns of EAMLs are varied and nonspecific. Therefore, the diagnosis of EAML is occasionally difficult, and EAMLs can be indistinguishable from high-grade or sarcomatous RCCs and AMLs with minimal fat. The heterogeneous enhancements

were caused by hemorrhaging, necrosis or fat components, and the majority of the solid tumors exhibited a tendency to be homogeneous on enhanced CT in the present study. In one of our series, the lesion was homogeneous on unenhanced CT but was enhanced heterogeneously and exhibited a peripheral enhancement pattern. To our knowledge, this finding has not previously been reported in the literature. Ten of the eleven solid tumors were markedly enhanced but were hypoattenuating relative to the renal cortex and medulla (arterial and venous phases), and this pattern is similar to the imaging findings for RCCs [13]. Lu et al. observed that centripetal enhancement that is homogeneous at the peak in addition to iso-enhancement in parenchymal phase might be the CEUS features of both EAMLs and minimal fat AMLs, but the pseudocapsule sign and tumor-to-cortex enhancement ratio were helpful in the differentiation between these conditions [8]. Only six patients underwent CEUS examinations in the present study, and all of the tumors were hypervascular. Two cases with a maximal tumor diameter of 8.0 cm were homogeneous, which might have resulted from uniform solid component without any hemorrhaging or necrosis. In RCCs, heterogeneous enhancement is most commonly observed using CECT or CEUS due to cystic changes, necrosis, or both [26, 27]. Thus, EAMLs should be a considered when a patient has a large mass that exhibits homogeneous enhancement on CEUS. Lesions containing hemorrhaging, necrosis and fat components are heterogeneous on CEUS, which is similar to the characteristics on enhanced CT.

The criteria for predicting malignant EAMLs are not well recognized because of the rarity of this entity. Large tumor size, necrosis, associated TSC or concurrent AML, extrarenal extension and/or renal vein involvement, a carcinoma-like growth pattern, frequent mitoses, a higher percentage of the epithelioid component and atypical mitotic figures might be associated with malignant outcomes [3, 23, 28]. One of our patients with associated TSC and a 10.2-cm mass accompany by necrosis in the upper polar relapsed 7 months after nephrectomy. Another patient developed distant metastasis in the adrenal gland 3 months after partial nephrectomy, but the lesion was not been biopsied. The 2004 World Health Organization classification

of tumors defines EAMLs as potentially malignant mesenchymal neoplasms with reported metastasis in approximately one-third of cases, but the true biological behavior of this rare variant remains unclear. In a multicenter clinicopathologic review of 40 cases, Brimo et al. found a 26% rate of malignancy [28]. Another multicenter clinicopathologic review of 41 cases by Nese et al., which included 16 previously published cases, described a 17% rate of recurrence and a 49% rate of metastasis, and 33% of the patients died due to the disease [3]. He et al. reported a series of 20 patients with a mean follow-up of 82.5 (range, 1-356) months, and only one patient developed distant metastases [7]. Moreover, Aydin et al. described benign clinical outcomes in all 15 of their patients [1]. This variability in clinical outcomes between reports could be related to the epithelioid component percentage, small sample sizes, and the sources of the cases (i.e., primary or referral pathology cases).

Several publications have observed functional activation of the mTOR pathway, and mTOR inhibitors, such as sirolimus and temsirolimus, can be used to treat TSCs associated renal EAMLs [29-31]. Therefore, the correct diagnosis of a renal EAML is important to help clinicians select the optimal treatment.

The present study has several limitations. First, only a small number of patients with EAMLs were included. Second, the long-term survival following this type of tumor awaits further research. Third, the epithelioid component percentages varied in our patients, which might have influenced the imaging appearances and clinic outcomes.

In conclusion, EAML is an uncommon tumor with the potential for aggressive, malignant behavior. Our data suggest that the majority of the tumors (size < 10 cm) were solid and exhibited a tendency toward being hyperattenuating on unenhanced CT images. The enhancement patterns were varied and nonspecific, and hemorrhaging or necrosis was found in tumors ≥ 10 cm with heterogeneous enhancement. Most of the solid tumors were markedly enhanced but were hypoattenuating relative to the renal cortex and medulla (arterial and venous phases). Regarding the CEUS appearances, the uniform lesions were hypervascular and homogeneous, whereas the lesions

that contained hemorrhaging, necrosis or fat components were heterogeneous.

## Disclosure of conflict of interest

None.

Address correspondence to: Cheng Liu, Department of Urology, The Second People's Hospital of Lianyungang, 161 Xingfu Road, Lianyungang 222-023, Jiangsu, China. Tel: (+86 518) 8577 5041; E-mail: Su-ga7858@126.com

## References

[1] Aydin H, Magi-Galluzzi C, Lane BR, Sercia L, Lopez JI, Rini BI and Zhou M. Renal angiomyolipoma: clinicopathologic study of 194 cases with emphasis on the epithelioid histology and tuberous sclerosis association. Am J Surg Pathol 2009; 33: 289-297.

[2] Luo J, Liu B, Wang Y, Li J, Wang P, Chen J and Wang C. Comprehensive clinical and pathological analysis of aggressive renal epithelioid angiomyolipoma: report of three cases. Onco Targets Ther 2014; 7: 823-827.

[3] Nese N, Martignoni G, Fletcher CD, Gupta R, Pan CC, Kim H, Ro JY, Hwang IS, Sato K, Bonetti F, Pea M, Amin MB, Hes O, Svec A, Kida M, Vankalakunti M, Berel D, Rogatko A, Gown AM and Amin MB. Pure epithelioid PEComas (so-called epithelioid angiomyolipoma) of the kidney: A clinicopathologic study of 41 cases: detailed assessment of morphology and risk stratification. Am J Surg Pathol 2011; 35: 161-176.

[4] Hornick JL, Fletcher CD. PEComa: what do we know so far? Histopathology 2006; 48: 75-82.

[5] Eble JN, Amin MB, Young RH. Epithelioid angiomyolipoma of the kidney: a report of five cases with a prominent and diagnostically confusing epithelioid smooth muscle component. Am J Surg Pathol 1997; 21: 1123-1130.

[6] Li J, Zhu M, Wang YL. Malignant epithelioid angiomyolipoma of the kidney with pulmonary metastases and p53 gene mutation. World J Surg Oncol 2012; 10: 1-5.

[7] He W, Cheville JC, Sadow PM, Gopalan A, Fine SW, Al-Ahmadie HA, Chen YB, Oliva E, Russo P, Reuter VE and Tickoo SK. Epithelioid angiomyolipoma of the kidney: pathological features and clinical outcome in a series of consecutively resected tumors. Mod Pathol 2013; 26: 1355-1364.

[8] Lu Q, Li CX, Huang BJ, Xue LY and Wang WP. Triphasic and epithelioid minimal fat renal angiomyolipoma and clear cell renal cell carcinoma: qualitative and quantitative CEUS characteristics and distinguishing features. Abdom Imaging 2015; 40: 333-342.

[9] Froemming AT, Boland J, Cheville J, Takahashi N, Kawashima A. Renal epithelioid angiomyolipoma: imaging characteristics in nine cases with radiologic-pathologic correlation and review of the literature. AJR Am J Roentgenol 2013; 200: W178-186.

[10] Bharwani N, Christmas TJ, Jameson C, Moat N, Sohaib SA. Epithelioid angiomyolipoma: imaging appearances. Br J Radiol 2009; 82: e249-252.

[11] Tsukada J, Jinzaki M, Yao M, Nagashima Y, Mikami S, Yashiro H, Nozaki M, Mizuno R, Oya M and Kuribayashi S. Epithelioid angiomyolipoma of the kidney: radiological imaging. Int J Urol 2013; 20: 1105-1111.

[12] Fang S, Dong D, Jin M. Perivascular epithelioid cell tumor (PEComa) of the kidney: MR features. Eur Radiol 2007; 17: 1906-1907.

[13] Bird VG, Kanagarajah P, Morillo G, Caruso DJ, Ayyathurai R, Leveillee R and Jorda M. Differentiation of oncocytoma and renal cell carcinoma in small renal masses (< 4 cm): the role of 4-phase computerized tomography. World J Urol 2011; 29: 787-792.

[14] Jung SC, Cho JY, Kim SH. Subtype differentiation of small renal cell carcinomas on three-phase MDCT: usefulness of the measurement of degree and heterogeneity of enhancement. Acta Radiol 2012; 53: 112-118.

[15] Kim JK, Kim TK, Ahn HJ, Kim CS, Kim KR, Cho KS. Differentiation of subtypes of renal cell carcinoma on helical CT scans. AJR Am J Roentgenol 2002; 178: 1499-1506.

[16] Shebel HM, Elsayes KM, Sheir KZ, Abou El Atta HM, El-Sherbiny AF, Ellis JH, El-Diasty TA. Quantitative enhancement washout analysis of solid cortical renal masses using multidetector computed tomography. J Comput Assist Tomogr 2011; 35: 337-342.

[17] Jinzaki M, Tanimoto A, Mukai M, Ikeda E, Kobayashi S, Yuasa Y, Narimatsu Y, Murai M. Double-phase helical CT of small renal parenchymal neoplasms: correlation with pathologic findings and tumor angiogenesis. J Comput Assist Tomogr 2000; 24: 835-842.

[18] Ruppert-Kohlmayr AJ, Uggowitzer M, Meissnitzer T, Ruppert G. Differentiation of renal clear cell carcinoma and renal papillary carcinoma using quantitative CT enhancement parameters. AJR Am J Roentgenol 2004; 183: 1387-1391.

[19] Young JR, Margolis D, Sauk S, Pantuck AJ, Sayre J, Raman SS. Clear cell renal cell carcinoma: discrimination from other renal cell carcinoma subtypes and oncocytoma at multiphasic multidetector CT. Radiology 2013; 267: 444-453.

[20] Sato K, Ueda Y, Tachibana H, Miyazawa K, Chikazawa I, Kaji S, Nojima T, Katsuda S. Malignant epithelioid angiomyolipoma of the kidney in a patient with tuberous sclerosis: an autopsy case report with p53 gene mutation analysis. Pathol Res Pract 2008; 204: 771-777.

[21] Fittschen A, Wendlik I, Oeztuerk S, Kratzer W, Akinli AS, Haenle MM, Graeter T. Prevalence of sporadic renal angiomyolipoma: a retrospective analysis of 61,389 in- and out-patients. Abdom Imaging 2014; 39: 1009-1013.

[22] Delgado R, de Leon Bojorge B, Albores-Saavedra J. Atypical angiomyolipoma of the kidney: a distinct morphologic variant that is easily confused with a variety of malignant neoplasms. Cancer 1998; 83: 1581-1592.

[23] Belanger EC, Dhamanaskar PK, Mai KT. Epithelioid angiomyolipoma of the kidney mimicking renal sarcoma. Histopathology 2005; 47: 433-435.

[24] Svec A, Velenska Z. Renal epithelioid angiomyolipoma--a close mimic of renal cell carcinoma. Report of a case and review of the literature. Pathol Res Pract 2005; 200: 851-856.

[25] Pea M, Bonetti F, Martignoni G, Henske EP, Manfrin E, Colato C, Bernstein J. Apparent renal cell carcinomas in tuberous sclerosis are heterogeneous: the identification of malignant epithelioid angiomyolipoma. Am J Surg Pathol 1998; 22: 180-187.

[26] Kim JK, Park SY, Shon JH, Cho KS. Angiomyolipoma with minimal fat: differentiation from renal cell carcinoma at biphasic helical CT. Radiology 2004; 230: 677-684.

[27] Xu ZF, Xu HX, Xie XY, Liu GJ, Zheng YL, Lu MD. Renal cell carcinoma and renal angiomyolipoma: differential diagnosis with real-time contrast-enhanced ultrasonography. J Ultrasound Med 2010; 29: 709-717.

[28] Brimo F, Robinson B, Guo C, Zhou M, Latour M, Epstein JI. Renal epithelioid angiomyolipoma with atypia: a series of 40 cases with emphasis on clinicopathologic prognostic indicators of malignancy. Am J Surg Pathol 2010; 34: 715-722.

[29] Wolff N, Kabbani W, Bradley T, Raj G, Watumull L, Brugarolas J. Sirolimus and temsirolimus for epithelioid angiomyolipoma. J Clin Oncol 2010; 28: e65-68.

[30] Shitara K, Yatabe Y, Mizota A, Sano T, Nimura Y, Muro K. Dramatic tumor response to everolimus for malignant epithelioid angiomyolipoma. Jpn J Clin Oncol 2011; 41: 814-816.

[31] Pan CC, Chung MY, Ng KF, Liu CY, Wang JS, Chai CY, Huang SH, Chen PC, Ho DM. Constant allelic alteration on chromosome 16p (TSC2 gene) in perivascular epithelioid cell tumour (PEComa): genetic evidence for the relationship of PEComa with angiomyolipoma. J Pathol 2008; 214: 387-393.